PAPER

NJC
www.rsc.org/njc

Spectroscopic properties and gelling ability of a set of rod-like 2,3-disubstituted anthracenes†

Jean-Pierre Desvergne,* Thierry Brotin, Danny Meerschaut, Gilles Clavier, Frédéric Placin, Jean-Luc Pozzo and Henri Bouas-Laurent*

Laboratoire de Chimie Organique et Organométallique (CNRS UMR 5802), Université Bordeaux 1, F-33 405, Talence cedex, France.
E-mail: jp.desvergne@lcoo.u-bordeaux1.fr

***Received* (in Montpellier, France) 17th June 2003, Accepted 6th October 2003**
First published as an Advance Article on the web 6th January 2004

The UV absorption spectra of 2,3-didecyloxyanthracene (DDOA) recorded in methanol, ethanol, 1-propanol, acetonitrile and methylcyclohexane reveal interesting features: they show a striking contrast between the isotropic solution and the gel state where, at ambient temperature, a fine structure appears with an apparent bathochromic shift ($\Delta\nu \approx -700$ cm^{-1}), as observed in the solid state. Such an effect was mimicked by 2,3-dioxydi- (and -tri-) methyleneanthracenes in which the conformational mobility of the two juxtanuclear oxygen atoms is reduced in a manner similar to that assumed in the gel state. The fluorescence emission of DDOA (10^{-5} M) at very low temperature exhibits a loss of fine structure and a bathochromic shift, for the gel state, in agreement with the presence of aggregates; the excitation spectra were found to be superimposable upon the absorption spectra of the isotropic and gel phases, respectively. Solvent screening for DDOA gelling ability has shown that the most efficient solvents are CH_3OH and CH_3CN. From the phase transition diagram (temperatures of gel setting, T_{gel}, and gel melting, T_m, *versus* concentration), thermodynamic parameters were derived: ΔH^0_{gel}/kJ mol^{-1} = −70 (CH_3OH), −66 (CH_3CN); ΔS^0_{gel}/(J K^{-1} mol^{-1} = −147 (CH_3OH), −140 (CH_3CN) and ΔG^0_{gel}/kJ mol^{-1} (at 300 K) ≈ −26 (CH_3OH), −24 (CH_3CN). These parameters attest to the good stability of these gel systems. Finally, the influence of the chain length ($n = C_7H_{15}$ to $C_{12}H_{25}$) on the efficiency of gel formation (or melting) was investigated in methanol, ethanol, acetonitrile and heptane. It emerges that, to form gels, *n*-decyl and *n*-undecyl were found to be the most suitable chains and methanol and ethanol the most efficient solvents. It should be noted that the ability to form gels in methanol at a concentration of 0.6 mM at ambient temperature qualifies DDOA as a supergelator.

Introduction

Gels are heterogeneous soft materials constituted of three dimensional (3D) networks imprisoning a liquid.[1–4] They are used in everyday life and continuous research efforts are being directed to extend their applications.[3–8]

For the last two decades, there has been a growing interest in gelation induced by the addition of low molar mass ($M \leq 1000$) substrates (the so-called LMOGs[9,27]) to organic liquids or, more rarely, water.[9–29] These compounds show a wide structural diversity. For convenience they can be classified into two categories: (1) gelators involving *hydrogen bonds*, ion-pairs or metal coordination and (2) systems involving *no H bonds* and based on van der Waals and weak electrostatic interactions. In the latter category, a comprehensive study has been devoted to the family of gelators containing steroidal and condensed aromatic rings, denoted ALS (aromatic linked steroids;[19] an example is shown in Scheme 1), whose discovery in 1987 gave a strong impetus to the development of the field.[19–49]

A few years later[28] some of us reported the gelling properties of 2,3-di-*n*-decyloxyanthracene (DDOA) for several organic solvents, especially methanol. Similarly to CAB (Scheme 1), it so happens that DDOA contains an anthracene nucleus that confers fluorescing properties onto the gels, but for DDOA, in contrast to the ALS family, the presence of alkoxy substituents

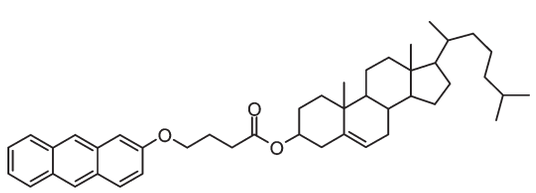

CAB

Scheme 1 Cholesteryl-4-(2-anthryloxy)butanoate (CAB), an example of the ALS family (see text); the presence of an anthracene containing tether was found to induce gelling properties and luminescence for a variety of organic liquids.[19]

in the 2 and 3 positions was found to be compelling for gelation to occur (Scheme 2). Furthermore, a rheological study[29] has shown that DDOA gels formed in 1-octanol could be described as soft solids exhibiting high yield stress values.

The elasticity of the DDOA gel ($G' \approx 10^4$ Pa at 1 wt %) was analysed as resulting from a 3D network of fibers or bundles of fibers with extended interaction zones, as borne out by small angle neutron scattering (SANS) investigations.[29] Various aspects of DDOA gel properties have been recently examined: aerogel formation in supercrital CO_2,[30] electrochemical properties in propylene carbonate,[31] porosity templating of sol-gel derived silica[32a] and alumina,[32b] gelation of liquid crystals.[33]

However, since the preliminary results,[28] no detailed spectroscopic study has been published. Such a study is reported here, together with a systematic exploration of the role played by the chain length ($R = C_nH_{2n+1}$) and an investigation of the

† Electronic supplementary information (ESI) available: UV absorption spectra of DDOA in 1-propanol and acetonitrile as a function of temperature; phase transition diagrams and related plots for DDOA in various solvents. See http://www.rsc.org/suppdata/nj/b3/b306961c/

DOI: 10.1039/b306961c

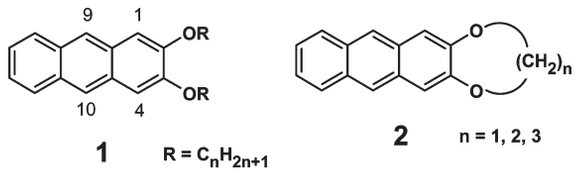

Scheme 2 2,3-Di-*n*-alkoxyanthracenes (DAOA) **1** and related heterocyclic compounds **2**. The compounds will be denoted $\mathbf{1}C_7$, $\mathbf{1}C_8$, *etc.* and $\mathbf{2}_1$, $\mathbf{2}_2$, $\mathbf{2}_3$, respectively. The di-*n*-decyloxy derivative (DDOA) was first shown to form a gel with alcohols and alkanes.[28]

thermodynamic parameters of the phase transitions (sol-to-gel and gel-to-sol).

Results and discussion

1. UV absorption and fluorescence spectroscopic properties of DDOA

The gelling property of DDOA was discovered through an unsuccessful crystallization in CH_3OH.[28] Subsequent rapid screening of gel-forming solvents showed that alcohol and alkanes are the best-suited. For this reason, the electronic absorption and emission spectra were studied essentially in methanol and methylcyclohexane (MCH); the latter was chosen for its ability to stay liquid at very low temperatures (m.p. −126 °C).

The absorption spectra of DDOA in CH_3OH are represented in Fig. 1. At 26 °C, the fluid isotropic solution exhibits the typical spectrum of 2,3-dialkoxy substituted anthracenes[50] but, at −15 °C, the medium is a translucent gel at the concentration used (10^{-3}M) and the spectrum appears to be strongly different. The first absorption band (300–400 nm), essentially constituted of the ^1L_a electronic transition, has a nice fine structure with well-defined vibronic maxima at 338, 347, 365 and 385 nm. The latter band, the most intense, shows an apparent bathochromic shift ($\Delta\nu \cong -700$ cm^{-1}); it probably corresponds to the 0-0 transition. This feature, combined with the enhanced fine structure as is the case for low temperature spectra, points to a great loss of freedom of orientation for the molecules in the gel. This statement is reinforced by the examination of the second band (200–300 nm), which, peaking as expected at 260 nm for the solution, shows a strong decrease of intensity in the gel; this change points to some parallelism between the long axes of the molecules due to π-π stacking.[51]

Typical spectra of the right angle fluorescence of a diluted solution of DDOA in methanol as a function of temperature are represented in Fig. 2. At 20 °C the spectrum resembles that of 2,3-dimethoxyanthracene taken as reference and its excitation spectrum is in line with that of Fig. 1. When the temperature is lowered, the gel forms and the fluorescence spectra are red-shifted, as usually seen for aggregates[52,53] and consistently the excitation spectrum becomes that of the gel as in Fig. 1.

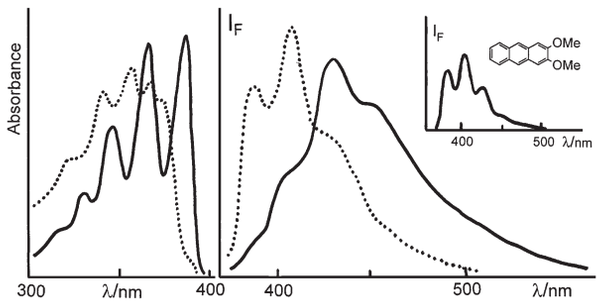

Fig. 2 Fluorescence and excitation spectra (arbitrary scale) of DDOA in degassed CH_3OH (10^{-4} M). Fluorescence λ_{exc}: 370 nm. Excitation: λ_{em}: 435 nm. 25 °C isotropic (···) and −70 °C gel (—) phases, respectively. Insert: Fluorescence spectrum of 2,3-dimethoxyanthracene in degassed ethanol ($\approx 3 \times 10^{-5}$ M) at −65 °C ($\lambda_{exc.}$: 365 nm), for comparison.

UV spectra of DDOA recorded in ethanol and 1-propanol *vs.* temperature [−15 °C (gel phase) to 20–50 °C (isotropic solution)] were found to show the same features as in methanol. An example of the spectra (300–400 nm) in 1-propanol (−15° to 26 °C) exhibiting clear isosbestic points is given as supplementary material (Fig. S1 in the ESI).

In methylcyclohexane (MCH), the fluorescence was studied from +20 °C to −104 °C. The fluorescence and excitation spectra of DDOA in degassed MCH at very low concentration (10^{-5} M) are represented in Fig. 3. The excitation spectrum of the gel shows a remarkably fine structure. The maximum wavelengths do not differ from those in CH_3OH. The emission spectrum of the gel is composed of "free" molecules dissolved in the imprisoned solvent and molecular aggregates immobilized *within* the fibrils, filaments and fibers, which experience different environments and therefore exhibit a variety of spectra as shown in the time-resolved spectra of Fig. 3 (insert). This is borne out by the results of a transient kinetic analysis, reported in Table 1. The *wavelength dependent* fluorescence decay can be fitted with a sum of two exponentials at all the wavelengths investigated. These decay times are all longer than that of the isolated molecule (≅ 4 ns) and are in agreement with the occurrence of different excited species displaying slightly different emission spectra, as recently discussed by De Schryver and coworkers[52,53] for anthracene chromophores

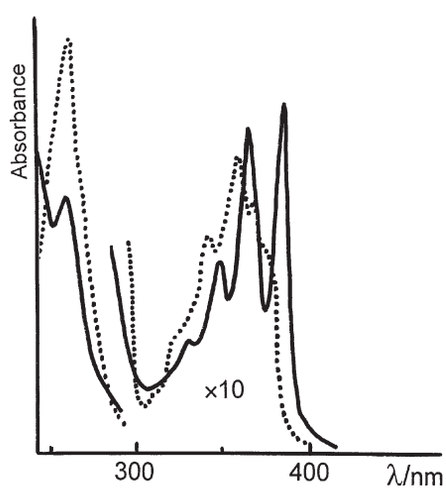

Fig. 1 Isotropic (···) and gel (—) phase absorption spectra of DDOA (≅10^{-3} M) in CH_3OH, at 26 °C and −15 °C, respectively.

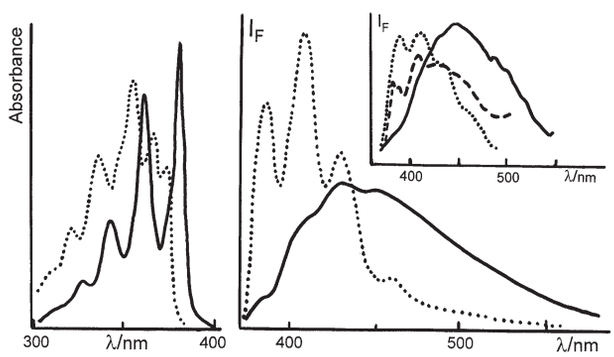

Fig. 3 Excitation (left) and fluorescence (right) spectra of DDOA (10^{-5} M) in degassed methylcyclohexane: solution (···) and gel (—). λ_{exc} 370 nm; λ_{obs} 410 nm (+20 °C) and 480 nm (−100 °C). Insert: time-resolved fluorescence spectra in MCH: +20 °C (···) 0 ns delay; −104 °C (---) 0 ns delay, −104 °C (—) 40 ns delay. The population of emitting aggregates changes with time.

Table 1 Fluorescence decay of DDOA ($\cong 8 \times 10^{-5}$ M) in degassed methanol at −45 °C. τ_1, τ_2 in ns; A_1 and A_2 are the preexponential factors of the fluorescence intensity decay: $I(t) = A_1\exp(-t/\tau_1) + A_2\exp(-t/\tau_2)$

λ_{obs}/nm	420	440	460	480
τ_1 (A_1)	5 (0.4)	8 (0.4)	9.5 (0.4)	11.5 (0.4)
τ_2 (A_2)	14 (0.14)	20 (0.07)	25 (0.05)	37 (0.04)
χ^2	1.44	1.09	1.05	1.32

in Langmuir–Blodgett films. The non-structured fluorescence spectra showing maximum intensity at 460 nm suggest the formation of excited aggregates from overlapping monomers as displayed by some non-sandwich overlapping excimers.[54]

The mutual arrangements of the anthracene nuclei in the gel are reminiscent of those in solid DDOA, as reflected in the compared UV spectra (Fig. 4). One might speculate about the correspondence between the crystal structure and the structure of aggregates in the gel as shown for instance by Terech,[9b] Weiss *et al.*[27a,b,41b] and Dastidar *et al.*[27c] but no distinct X-ray diffractograms could be obtained on pure DDOA gels and we never could grow any single crystals of DDOA. In the series the only single crystals suitable for X-ray determination were obtained for di-*n*-hexyloxyanthracene (DHOA),[55] but no X-ray studies were performed on the gels of DHOA. The question of the structure at the molecular level has been addressed in a recent paper showing some unique features of the gel phase.[56]

The UV absorption spectrum of the gel phase does not depend on the gelling solvent and it was used to follow-up the gel formation of DDOA in a matrix of silica gel.[32a] Such a gel could be formed from $Si(OCH_3)_4$ (TMOS), methanol, water and a base (to obtain pH 12.7) by adding a methanolic solution of DDOA (10^{-3}M) and heating at 50 °C for several minutes, then allowing to cool down to ambient temperature. Under these conditions, the inorganic gel was formed first, followed by gradual formation of the organic gel. The inclusion of the DDOA gel could be traced by recording the UV spectra as a function of temperature (Fig. 5).

The UV absorption spectra of a solution of DDOA in CH_3CN (6×10^{-4}M) was recorded as a function of temperature (2.4 °C to 50 °C) and showed the same characteristic changes (including isosbestic points) as observed in methanol and 1-propanol (Fig. S2 in the ESI).

The difference in the vibronic structure between the isotropic solutions (in methanol, MCH or acetonitrile) and the gel (and the solid state) might be in line with the ability of oxygen lone pairs to align parallel with the π electrons of the anthracene nucleus. A qualitative piece of evidence to support this hypothesis comes from a comparison of the UV absorption spectra of the heterocyclic derivatives $\mathbf{2}_{1,2,3}$ with those of the acyclic compounds $\mathbf{1}_{CH3}$ and $\mathbf{1}_{C10}$ (see Fig. 6). The acyclic compounds exhibit λ_{max} 374–376 nm, irrespective of the solvent and the chain length. It thus reflects an average orientation of the

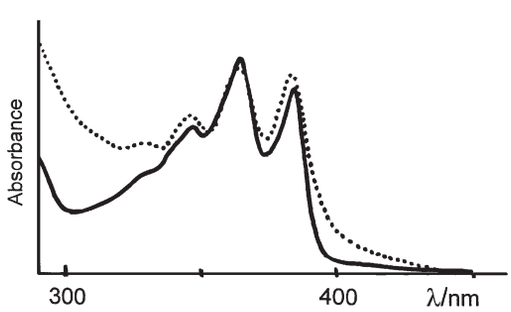

Fig. 4 UV absorption spectra of DDOA in a KBr pellet (···) and of its gel (—) in methanol at ambient temperature. The diffused light is more important in KBr.

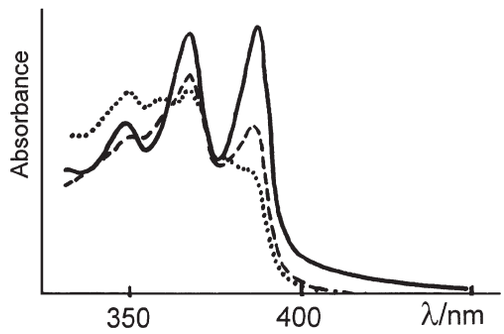

Fig. 5 UV absorption spectra of DDOA in a silica gel matrix in a 1 mm quartz cell as a function of temperature: (—) 25 °C (organogel), (---) 40 °C (mixture of organogel and isotropic phase), (···) 45 °C (the same mixture with a higher proportion of isotropic phase).

freely rotating oxygen atoms; this is strongly inhibited in the methylenedioxy compound $\mathbf{2}_1$, which results in an hypsochromic shift (370 nm). In contrast, the propylenedioxy substituent in $\mathbf{2}_3$ induces a bathochromic shift (382 nm); another red shift (390 nm) is exhibited by the six-membered ring compound $\mathbf{2}_2$ in which the oxygen atoms appear to be maintained in the best geometry for conjugation. From these data, it emerges that, in the gel, the oxygen atoms should have a geometry intermediate between those of 2,3-propylenedioxyanthracene ($\mathbf{2}_3$) and 2,3-ethylenedioxyanthracene ($\mathbf{2}_2$).

2. Photochemical reactivity of DDOA

Anthracenes are known to have photochromic properties[57] but our attempts to confer this property to the DDOA gels met with failure. No clear change was noted after 2 h irradiation of a methanolic gel in a Pyrex tube with a medium pressure mercury lamp. The photoreactivity of DDOA was thus investigated in isotropic solution. Irradiation of a degassed benzene solution (10^{-3} M) with a medium pressure mercury lamp, using a Pyrex filter, was followed by UV spectroscopy. The

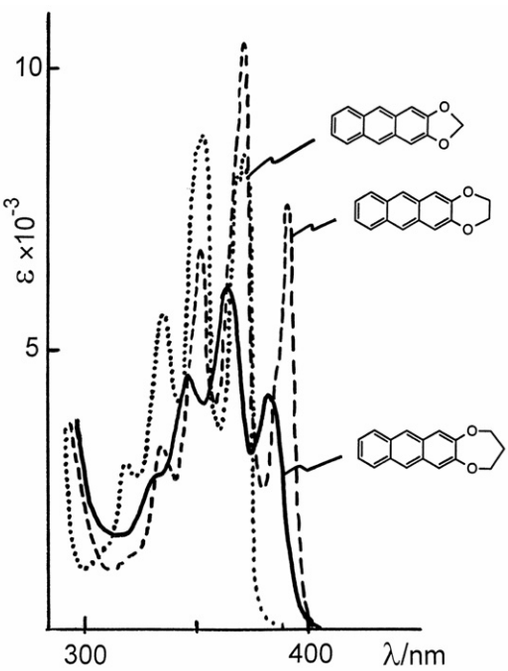

Fig. 6 UV absorption spectra, at ambient temperature, in MCH ($c \cong 10^{-4}$6 M) of 2,3-methylenedioxyanthracene ($\mathbf{2}_1$), 2,3-ethylenedioxyanthracene ($\mathbf{2}_2$) and 2,3-trimethylenedioxyanthracene ($\mathbf{2}_3$). The onset wavelength increases from 370 to 382 to 390 nm for $\mathbf{2}_1$, $\mathbf{2}_3$ and $\mathbf{2}_2$, respectively.. Compare these UV spectra with those of Figs. 1–4.

300–400 nm absorption slowly disappeared while another absorption band, at $\lambda < 300$ nm tailing down to 450 nm, grew in after 14 h. After allowing the solution to stand for 12 h, the UV spectrum of DDOA was recovered. Attempts to isolate the photoproduct(s) were unsuccessful. No definite products could be obtained either from irradiation in the presence of oxygen. As a result of their photoreactivity, it is advisable to keep the gels in the dark and under inert gas. Under these conditions, methanolic gels ($\approx 5 \times 10^{-3}$ M) were found to be stable for more than one year.

3. Solvent screening for gel-forming ability

DDOA was found to form gels in methanol *at ambient temperature* at a concentration as low as 6×10^{-4} M (0.04 wt %). Most gels are known to be formed at a concentration of *ca.* 1 wt %; the efficiency of DDOA in methanol is therefore outstanding (comparable values for supergelators were reported by others[35e,46a]) and systematic tests of gel-forming solvent ability were undertaken using the inverted tube method described in the Experimental. Some salient results are collected in Table 2; the molar concentration was chosen with a view to obtaining thermodynamic data (see Section 4) and as a common basis for comparison between the different 2,3-dialkoxyanthracenes. It is remarkable that, in many cases, gels can be formed at concentrations as low as 10^{-3} M. One observes that alcohols and alkanes are less easily gelified by DDOA as the molecular weight increases. Among alcohols, gel-forming ability decreases with branching (*e.g.* butane-2-ol *vs.* 1-butanol); however, 2,3-butanediol behaves like ethanol. Acetonitrile shows good performance but the solubility is limited to 10^{-2} M. For potential applications to electrochemistry, propylene carbonate was found to deserve special study[31] and the methacrylates were tested for possible polymerization using DDOA gel as a template.[11,12] It is also worth noting that supercritical CO_2 (not reported in Table 2) was explored as a solvent to produce aerogels,[30] as mentioned in the Introduction.

DDOA is not soluble in water but addition of some water to alcohols was found to be possible, as shown in silica sol gels using DDOA gel as a template[32] and as experienced with other gelators[58,59] (see Section 1). DDOA was found to be very soluble in CH_2Cl_2 and $CHCl_3$ at ambient temperature; addition of methanol or ethanol to such solutions allows formation of gels; however, this method was not explored further.

Table 2 Organic solvents tested for gelation of DDOA at low concentration[a] by the inverted tube method:. (+) denotes gel formation and (−) no gel formation observed

Solvent	Concentration/M	Ambient temperature	−18 °C
Methanol	6×10^{-4}	+	
Ethanol	1×10^{-3}	+ (8–10 °C)	
1-Propanol	1.7×10^{-3}	+ (0 °C)	
2-Propanol	1.2×10^{-3}	−	+
1-Butanol	2×10^{-3}	+ (0 °C)	
2-Butanol	1.3×10^{-2}	−	+
2,3-Butanediol	1.1×10^{-3}	+	
1-Octanol	10^{-2}	+	
Propylene carbonate	10^{-2}	+	
n-Pentane	2.8×10^{-3}	−	+
n-Hexane	5×10^{-3}	+	
n-Heptane	10^{-2}	+	
Isooctane	10^{-2}	+	
Acetonitrile[b]	7.5×10^{-4}	+	
Acetone	3×10^{-3}	−	+
DMF	1.1×10^{-3}	−	+
DMSO	1.4×10^{-3}	+	
Methyl methacrylate	10^{-2}	+	
Lauryl methacrylate	10^{-2}	+	

[a] Concentration in mol (M) was adopted as it is used in thermodynamics (see phase transition diagrams below). [DDOA] in CH_3OH (molar mass: 490): 5×10^{-4} M = 0.03 wt %; 10^{-3} M = 0.06 wt %; 10^{-2} M = 0.62 wt % [b] Solubility limited to 10^{-2} M

4. Phase transition diagrams and thermodynamic parameters

In order to gain more insight into the efficiency of gel formation and the melting of DDOA, phase transition temperatures were measured as a function of concentration in methanol, ethanol, heptane, acetonitrile and propylene carbonate. The temperatures [T_m (gel melting) and T_{gel} (gel formation)] were measured with an accuracy of ±0.5 °C, using a thermostatted bath (heating and cooling rates of 1.5 °C min^{-1}) and an automated apparatus allowing the registration of transmittance of the diffused light. (see Experimental). As the dimensions of the fibers are of the same order of magnitude as the visible light wavelengths, the diffused light intensity increases with their concentration. These measurements seem to be less arbitrary than those based on mechanical tests of gelification.

Phase transition diagrams. A typical phase transition diagram, that of DDOA in methanol, is presented in Fig. 7, accompanied by the thermodynamic correlation expressed in eqns (1) and (2) below (see Fig. 8). In this solvent, the maximum temperature is limited by the boiling point of methanol (64.5 °C); it is thus useless to increase the DDOA concentration to increase T_m. In principle, the maximum gelification temperature should not exceed the melting point of the gelator (m.p. DDOA 87 °C). One notes a clear hysteresis between the melting and gelification processes; this phenomenon depends on the temperature variation rate and points to the difficulty in characterizing a reversible process dealing with partial heterogeneity. The temperatures of gelification (T_{gel}) were observed to vary very little between different experiments whereas the melting temperatures (T_m) depend on the thermal history of the sample.

Gel formation can be assumed to resemble a crystallization; thus, it will be described by the following thermodynamic equations (see Appendix):

$$\text{Gel melting}: \ \ln\phi = -\Delta H^0/R \times 1/T_m + \Delta S^0/R \quad (1)$$

$$\text{Gel formation}: \ \ln\phi = +\Delta H^0/R \times 1/T_{gel} - \Delta S^0/R \quad (2)$$

ΔH^0 and ΔS^0 are positive for the melting and negative for the gelification processes, respectively; ϕ denotes the molar fraction of the solute in the appropriate solvent (see Appendix).

The diagram for gelification of DDOA in *n*-heptane (Fig. 9) clearly shows that the concentrations used are much higher than in methanol (as qualitatively suggested in Section 3). It is accompanied with the linear plot according to eqn. (2) (see Fig. 10). Other diagrams (Fig. S3a–d) and linear graphs

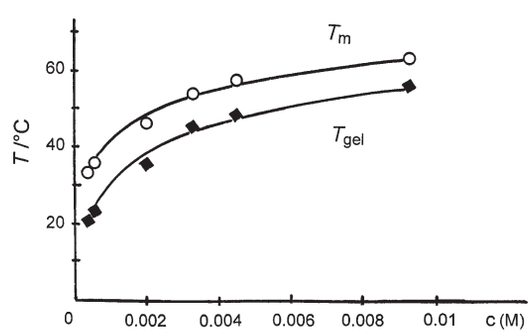

Fig. 7 Phase transition diagram of DDOA in methanol. T_m and T_{gel} denote the gel-to-sol and the sol-to-gel transition temperatures, respectively. A hysteresis with $\Delta T \approx 10$ °C was observed. T accuracy ±0.5 °C.

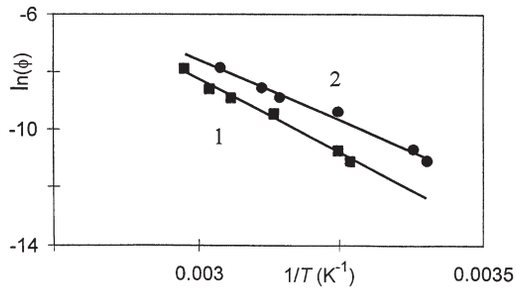

Fig. 8 $\ln\phi$ *vs.* $1/T$ plots for DDOA in methanol, showing a good linearity ($r^2 = 0.987$). 1 represents the gel-to-sol transition and 2 the sol-to-gel process. See eqns (1) and (2).

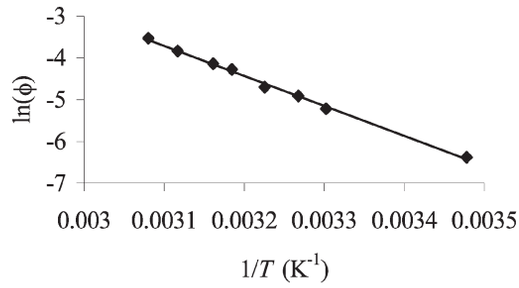

Fig. 10 $\ln\phi$ *vs.* $1/T$ plot for DDOA gelification in *n*-heptane [eqn. (2)].

(Fig. S4a–c) obtained in *n*-heptane, acetonitrile and propylene carbonate are given as supplementary material.

From these data, the thermodynamic parameters ΔH^0 and ΔS^0 were calculated and are listed in Table 3. Are also included the values obtained from a study of 2,3-dialkoxyanthracenes incorporating chains of different lengths (*vide infra*). From the upper part of Table 3, it emerges that *n*-heptane seems to have a lower ability to form gels with DDOA (the free enthalpy at 27 °C clearly has a lower value) than the other solvents, presumably because of a better solvation power. On the other hand, methanol appears to be the most appropriate solvent.

Influence of the chain length on the gelification efficient. After discovering the gelling ability of DDOA and having shown that it is connected to the presence of two alkoxy chains in positions 2 and 3 of anthracene, an obvious question was that of the *optimum* chain length. The whole series of derivatives **1**(C_6–C_{12}) was prepared and preliminary tests show that **1**C_6 could not give gels at room temperature but provided single crystals suitable for X-ray structure determination.[55] The other compounds formed gels in alcohols, though it is noted that **1**C_7 was clearly borderline and **1**C_{12} looked less efficient in ethanol. Phase transition diagrams were therefore established for **1**C_8–**1**C_{11} in ethanol (see Figs. 11 and 12) and the thermodynamic parameters were determined (Table 3). Despite some discrepancies in the enthalpy and entropy values, the free enthalpies show a trend of increasing stability (at 27 °C) from **1**C_8 to **1**C_{11} but the differences are rather small.

Another appraisal of the chain length influence can be obtained from the melting temperatures (although these are less reliable than the gelification temperatures, they can be easily determined by the inverted tube method) for a fixed concentration (10^{-2} M) in different solvents, as shown in Fig. 13. In methanol, ethanol and acetonitrile, **1**C_{10} and **1**C_{11} behave as the most efficient compounds if one uses the melting temperature as the main criterion.

The data of Table 3 are to be compared with the published thermodynamic values of other LMOGs. Some of these have been selected for a variety of gelators and are listed below; most of them (except for the cholesterol-based systems) are of the H-bonded type. Shinkai and coworkers[60] determined the melting enthalpy for a number of derivatives (differing in the alkoxy group) of para-alkoxy-substituted azobenzene-appended cholesterol-based gelators (αC-3): $41 < \Delta H^0_m/\text{kJ mol}^{-1} < 160$ in ethanol and $41 < \Delta H^0_m/\text{kJ mol}^{-1} < 110$ in 1-butanol. For *N*-benzoyloxycarbonyl-L-alanine-4-hexadecanoyl-2-nitrophenyl esters (BLAHN), Hanabusa and coworkers[61] reported $\Delta H^0_{gel} = -23$ and -25 kJ mol^{-1}, $\Delta S^0_{gel} = -7$ and -10 J K^{-1} mol^{-1}and ΔG^0_{gel} (at 300 K) $= -21$ and -22 kJ mol^{-1}, in methanol and cyclohexane, respectively. In addition, a more substituted derivative of the same family exhibited the following parameters in cyclohexane: $\Delta H^0_{gel} = -42$ kJ mol^{-1}, $\Delta S^0_{gel} = -56$ J K^{-1} mol^{-1} and ΔG^0_{gel} (at 300 K) $= -26$ kJ mol^{-1}. Garner, Terech and coworkers[15] have derived the parameters for the trans isomer of 4-*tert*-butyl-1-phenylcyclohexanol (BACOl) in several solvents: $\Delta H^0_m = 35.6$ and 28.5 kJ mol^{-1} and $\Delta S^0_m = 75.5$ and 66 J K^{-1} mol^{-1}; hence the free enthalpies at 300 K are $\Delta G^0_m = 13.5$ and 9.2 kJ mol^{-1}, in n-heptane and dichloromethane, respectively. Typical values of gel formation enthalpies for hexose derivatives were derived by Shinkai and coworkers:[62] for α-1-*O*-methyl-4,6-*O*-benzylidene-D-glucose $\Delta H^0_{gel}/\text{kJ mol}^{-1} = -43$ (toluene), -40 (tetrachloromethane) whereas for the D-galactose isomer $\Delta H^0_{gel}/\text{kJ mol}^{-1} = -40$ (toluene), -45 (tetrachloromethane). Interestingly, for some dithienylcyclopentenediamides in toluene ΔH^0_m values of up to 98 kJ mol^{-1} were found, presumably due to a strong H-bond network.[63]

The enthalpy values reflect the network strength and the importance of the entropy in the phase transition is clearly

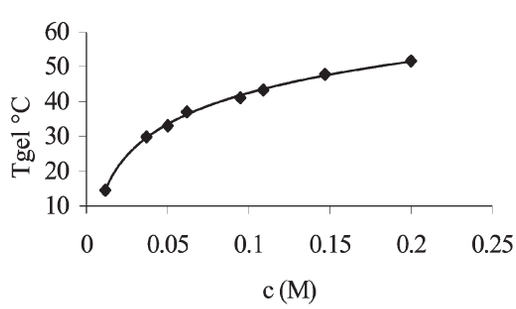

Fig. 9 Phase transition diagram for the gelification of DDOA in *n*-heptane. Temperature accuracy: ±0.5 °C.

Table 3 Thermodynamic parameters (ΔH^0, ΔS^0) obtained from the phase transition diagrams (T_{gel} or T_m *vs.* concentration) and free enthalpy (ΔG^0) at 300 K in CH_3OH, *n*-heptane, CH_3CN and propylene carbonate for DDOA. In EtOH, the parameters were determined for compounds with different chain lengths. Accuracy on ΔH^0 and ΔS^0 is ±10%

Solvent and compound	ΔH^0/kJ mol^{-1}		ΔS^0/J K^{-1} mol^{-1}		ΔG^0 (27 °C)/kJ mol^{-1}	
	Gelif.	Melting	Gelif.	Melting	Gelif.	Melting
Methanol						
1C_{10}	−70	+86	−147	+188	−25.9	+29.5
b-Heptane						
1C_{10}	−60	+92	−155	+246	−13.5	+18.2
Acetonitrile						
1C_{10}	−66	+72	−140	+152	−24.0	+26.4
Propylene carbonate						
1C_{10}	−58	–	−115	–	−24.5	–
Ethanol						
1C_8	−52	+74	−103	+165	−21.1	+24.5
1C_9	−53	+85	−104	+190	−21.8	+28.0
1C_{10}	−64	+93	−139	+218	−22.3	+27.6
1C_{11}	−48	+81	−82	+171	−23.4	+29.7

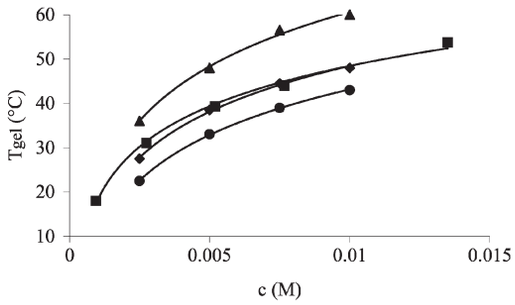

Fig. 11 Phase transition diagram for the gelification of **1**(●C_8, ◆C_9, ■C_{10}, ▲C_{11}) in EtOH. Temperature accuracy: ±0.5 °C.

apparent. The data listed in Table 3 compare well with those reported above and attest to a good stability of DDOA gels in methanol, ethanol and acetonitrile.

Differential scanning calorimetry. This technique is generally used to determine phase transition temperatures and enthalpies. Measurements effectuated on pure DDOA powder for the melting and resolidification led to a m.p. of 87.7 °C and $\Delta H^0_m = 42$ kJ mol^{-1} while the solidification point is 87.1 °C with $\Delta H^0_{solid} = 37$ kJ mol^{-1}. Because methanol has a relatively low melting point, propylene carbonate (boiling point at 1 bar of 240 °C) was chosen to measure gel transition temperatures. The thermograms are shown in Fig. 14. The transition enthalpies were determined to be $\Delta H^0_m = 65$ kJ mol^{-1} and $\Delta H^0_{gel} = -37$ kJ mol^{-1}. Although one finds a hysteresis gap of about 10 °C, as in the preceding measurements based on diffused light, the gelification temperature (≈ 55 °C) is different from that found with the automated apparatus (≈ 60 °C, Fig. S_3d in ESI). The discrepancy observed for the ΔH^0_{gel} values in propylene carbonate (−58 kJ mol^{-1} reported in Table 3) and the above value (−37 kJ mol^{-1} obtained by DSC) is not clearly understood. Moreover, we cannot offer a satisfactory explanation for the fact that ΔH^0_m was found to be 42 kJ mol^{-1} (DDOA powder) and 65 kJ mol^{-1} (gel in propylene carbonate). The DSC method should be applied to all samples under various heating and cooling rates. These thermodynamic data should be considered as preliminary.

Summary and conclusions

In exploring further the spectroscopic properties of DDOA (**1**C_{10}), this study has revealed that the UV spectra of the gel state exhibits a clear fine structure and an apparent bathochromic shift (≈−700 cm^{-1}) irrespective of the solvent used (methanol, ethanol, 1-propanol, acetonitrile, methylcyclohexane or *n*-heptane). It is suggested that these features are induced by a reduced mobility of the conformation of the juxtanuclear oxygen atoms, as in 2,3-dioxydi- (and -tri-) methyleneanthracenes. The remarkable gel-forming properties of DDOA (in methanol, at 20 °C, at 6×10^{-4} M = 0.04 wt %)

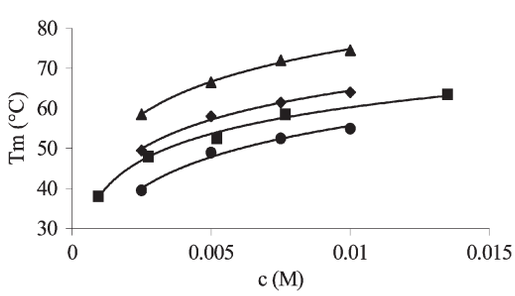

Fig. 12 Phase transition diagram for the melting of **1**(●C_8, ◆C_9, ■C_{10} and ▲C_{11}) in EtOH. Temperature accuracy: ±0.5 °C.

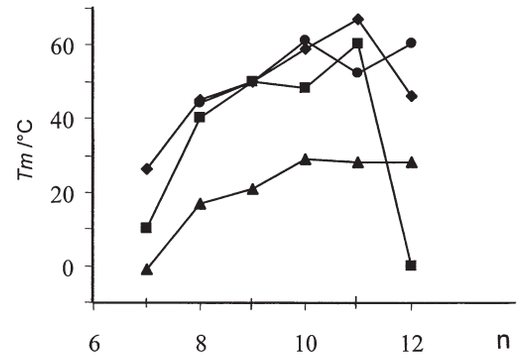

Fig. 13 Gel melting temperatures (T_m) as a function of the chain length in **1**(C_7–C_{12}) at $c = 10^{-2}$ M in ●methanol, ◆ethanol, ■acetonitrile and ▲*n*-heptane.

were also observed in other members of the family with R = C_7H_{15} to $C_{12}H_{25}$, in ethanol, acetonitrile and heptane; **1**C_{10} and **1**C_{11} were found to be the most efficient gelators and *n*-heptane the least appropriate solvent. A test of solvent efficiency was obtained by plotting the phase transition temperature diagram *versus* concentration; from these diagrams, the thermodynamic parameters ΔH^0_m , ΔS^0_{gel} and ΔS^0_m (gel denotes gel formation and m is for melting) that have been determined are in keeping with a good stability of these systems in alcohols and acetonitrile and a fair stability in *n*-heptane. The present results confirm and extend previous work on DDOA. Other recent studies dealing with infrared spectra and polarized fluorescence spectra of aerogels help in getting a deeper insight into the gel structure at the molecular level.[56]

Experimental

General methods and materials

Melting points were determined in capillary tubes on a Buchi 510 apparatus and are uncorrected. FTIR spectra were recorded on a Perkin Elmer Paragon 1000 spectrophotometer. ^{1}H NMR spectra at 250 MHz and ^{13}C NMR spectra at 62.9 MHz were recorded on a Bruker 250 AC instrument for solutions in $CDCl_3$ unless stated otherwise. Chemical shifts are given in ppm and *J* values are given in Hz. Chromatographic separations were performed on SDS silica chromagel (70–210 μm). Mass spectra were obtained on an AutoSpeq EQ spectrometer. Elemental analyses were performed by the Microanalytical Service, Institut du Pin, University Bordeaux I. Electronic absorption spectra and transmission spectra were measured on

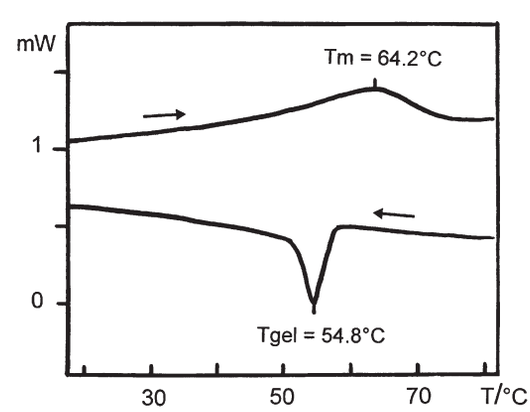

Fig. 14 Differential scanning calorimetry of a 10^{-2} M solution of DDOA in propylene carbonate: heating (→) and cooling (←) rates of 5 °C min^{-1}.

an Hitachi U-3300 spectrophotometer equipped with a thermocontrolled cell monitored by a Lauda thermostat. The measurements were realized using cells having 10 mm optical pathlength and a platinum temperature sensor. For differential scanning calorimetry measurements, a Perkin Elmer DSC 7 equipped with a stainless steel capsule having a rubber O-ring was used.

The temperature-dependent fluorescence emission and excitation spectra were obtained on a Hitachi F-4500 fluorescence spectrophotometer corrected for excitation and emission using quartz cells with a 1 cm optical pathlength, which were placed in a copper holder inside a quartz Dewar flushed with cold nitrogen gas. The temperature was adjusted by the nitrogen flow. The fluorescence decays were measured by single photon counting (Applied Photophysics) as described elsewhere.[64] Spectroscopic grade solvents were used for spectrophotometric measurements. No fluorescent contaminants were detected upon excitation in the wavelength region of experimental interest. The samples were degassed by freeze-pump-thaw cycles on a high-vacuum line and sealed under vacuum.

Solvents used for synthesis and gelation tests (alcohols, alkanes, acetonitrile, acetone, DMF, DMSO, propylene carbonate, methyl and laurylmethacrylate, *etc.*) were purchased from SDS (Peypin, Bouches du Rhône, France) and are of synthesis grade. Solvents of spectroscopic grade (methanol, ethanol, 1-propanol, acetonitrile, heptane, methylcyclohexane, *etc.*) from Aldrich were used for UV and fluorescence studies.

Gelation tests

In a typical gelation experiment, 1 cm^3 of solvent of special grade was added to a weighed amount of gelator in a septum-capped test tube (*ca.* 4 cm length and 0.7 cm diameter) in order to obtain the desired concentration. The mixture was warmed to the boiling point until the solid was dissolved and then was allowed to cool down to room temperature. In those cases in which a gel was formed, which generally occurred within several minutes and was confirmed by observing that the sample did not flow *when the test tube was inverted*, the tube was weighed to quantify the amount of gelatinized solvent. When the solution was turbid but the solvent was not entirely gelatinized, the mixture was warmed again and then cooled in a freezer (−18 °C) for 24 h.

Phase transition temperature measurements

The measure of temperatures was based on the variation of diffused visible light intensity as a function of the temperature, using an automated apparatus, as described elsewhere.[31] The monitoring light was that of a laser diode beam, at 670 nm, a wavelength at which the samples do not absorb, and the transmitted light was measured by a photodiode. The heating/cooling cycles were performed at a rate of 1 °C min^{-1} and repeat measurements (at least 3 per compound) indicate that the phase transition temperatures [T_{gel} (sol → gel) and T_m (gel → sol)] could be determined with an accuracy of ±0.5 °C. A hysteresis was systematically observed (see Fig. 15 for a typical diagram), related to the existence of an enthalpy for the sol-gel transition and its magnitude depends on the heating/cooling rates.

Preparations

Compounds **1**(C_1 and C_7–C_{12}) and $\mathbf{2}_{1-3}$, studied in this article, have been synthesized from a common substrate: 2, 3-dihydroxyanthraquinone (**4**), as outlined in Scheme 3.

The preparations of **4** (m.p. 393–394 °C, sublim.), **1**C_1 (m.p. 133 °C), **1**C_{10} (m.p. 84 °C) and **1**C_{12} (m.p. 74 °C) were described in a preceding publication.[50] Compounds $\mathbf{2}_1$ (m.p. 250–252 °C) and $\mathbf{2}_2$ (m.p. 204–205 °C) are known.[65] In the following, the preparations of **1**(C_7, C_8, C_9 and C_{11}) and $\mathbf{2}_3$ are detailed.

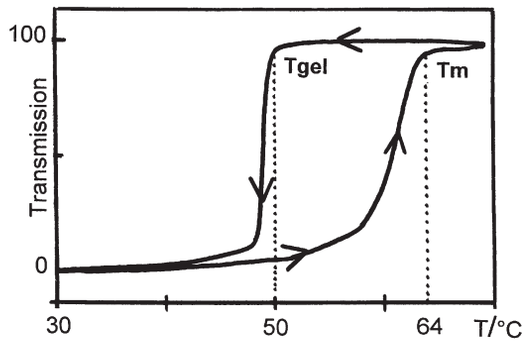

Fig. 15 Typical light transmission diagram as a function of temperature (variation 1 °C min^{-1}) as recorded by the self-monitoring set-up.[31]

Compounds 3C_n: general procedure for the alkylation of 2,3-dihydroxyanthraquinone. In a three-neck round-bottom flask equipped with a reflux condenser and a dropping funnel, the required amount of **4** and potassium carbonate (2.5 molar equiv. per hydroxy group) were added to freshly distilled DMF (10 cm^3 per mmol of **4**); the medium was warmed until complete dissolution then the appropriate alkylbromide (2.25 molar equiv. per hydroxy group) was added dropwise over 20 min. The reaction mixture was refluxed for 12 h before being allowed to cool to room temperature. The solvent was evaporated under reduced pressure and the residue was treated with water and thoroughly extracted with dichloromethane. The organic layers were combined, dried ($MgSO_4$) and filtered; the solvent was evaporated and the raw solid was chromatographed on a column of silica gel after dissolution in one of the following eluting mixtures of CH_2Cl_2–petroleum ether (v/v): (A) 20:80; (B) 40:60. Average yields were 80–85%.

*2,3-Diheptyloxy-9,10-anthraquinone (***3C_7***).* Starting from 1.5 g of **4**, compound **3**C_7 (2.4 g, 88%), m.p. 92 °C (methanol), was isolated with elution system B. Anal. calcd for $C_{28}H_{36}O_4$: C, 77.03; H, 8.31%; found: C, 76.92; H, 8.37%. ν_{max} (KBr): 3076, 2956, 2924, 2854, 1669, 1577, 1514, 1466, 1377, 1332, 1312, 1219, 1111, 1087, 713 and 621 cm^{-1}. ^{1}H NMR ($CDCl_3$): δ 8.16 (2H, m, H5 and H8); 7.65 (2H, m, H6 and H7); 7.55 (2H, s, H1 and H4); 4.11 (4H, t, $J = 6.7$ Hz, OCH_2); 1.85 (4H, m, OCH_2CH_2); 1.47 (4H, m, $OCH_2CH_2CH_2$); 1.21 (12H, m); 0.87 (6H, t, $J = 6.7$ Hz, CH_3). ^{13}C NMR: δ 182.4 (C9 and C10); 153.7 (C2 and C3); 133.6 (C6 and C7); 133.5 (C8a and C10a); 128.0 (C4a and C9a); 126.8 (C5 and C8); 109.2 (C1 and C4); 69.3 (OCH_2); 31.8 ($CH_2CH_2CH_3$); 29.0 (t); 28.9 (t); 25.9 (t); 22.6 (CH_2CH_3); 14.1 (CH_3).

*2,3-Di-n-octyloxy-9,10-anthraquinone (***3C_8***).* Starting from 1.5 g of **4**, compound **3**C_8 (2.45 g, 85%), m.p. 97 °C (methanol),

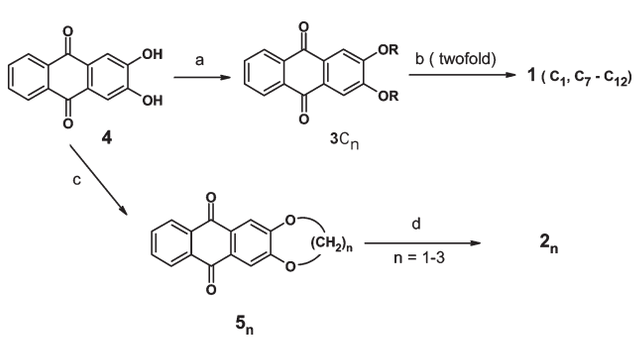

Scheme 3 Synthetic pathways for the preparation of **1**(C_1, C_7–C_{12}) and $\mathbf{2}_{1-3}$: (a) RBr, DMF, K_2CO_3; (b: i) $NaBH_4$, EtOH; (b: ii) HCl; (c) $Br(CH_2)_nBr$, DMF, K_2CO_3; (d) Zn, NH_4OH.

was isolated with elution system B. ν_{max} (KBr): 3076, 2921, 2851, 1671, 1576, 1515, 1465, 1377, 1332, 1315, 1220, 1111, 1087 and 712 cm^{-1}. ^1H NMR ($CDCl_3$): δ 8.15 (2H, m, H5 and H8); 7.65 (2H, m, H6 and H7); 7.55 (2H, s, H1 and H4); 4.11 (4H, t, $J = 6.7$ Hz, OCH_2); 1.85 (4H, m, OCH_2CH_2); 1.47 (4H, m, $OCH_2CH_2CH_2$); 1.30–1.20 (16H, m, CH_2); 0.86 (6H, t, $J = 6.7$ Hz, CH_3). ^{13}C NMR: δ 182.4 (C9 and C10); 153.7 (C2 and C3); 133.6 (C6 and C7); 133.5 (C8a and C10a); 128.0 (C4a and C9a); 26.8 (C5 and C8); 109.2 (C1 and C4); 69.3 (OCH_2); 31.8 (t); 29.3 (t); 29.0 (t); 25.9 ($OCH_2CH_2CH_2$); 22.7 (OCH_2CH_3); 14.1 (CH_3). FAB^+-MS: m/z (%) 464 (100), 353 (44), 240 (85).

*2,3-Di-n-nonyloxy-9,10-anthraquinone (**3**C_9).* Starting from 1.0 g of **4**, compound **3**C_9 (1.75 g, 85%), m.p. 103—104 °C (methanol), was isolated with elution system B. ν_{max} (KBr): 3078, 2957, 2920, 2850, 1670, 1575, 1514, 1466, 1332, 1220, 1111, 712 et 621 cm^{-1}. ^1H NMR ($CDCl_3$): δ 8.17 (2H, m, H5 and H8); 7.66 (2H, m, H6 and H7); 7.59 (2H, s, H1 and H4); 4.13 (4H, t, $J = 6.7$ Hz, OCH_2); 1.82 (4H, m, OCH_2CH_2); 1.45 (4H, m, $OCH_2CH_2CH_2$); 1.30–1.20 (20H, m, CH_2); 0.83 (6H, t, $J = 6.7$ Hz, CH_3). ^{13}C NMR: δ 183.1 (C9 and C10); 153.5 (C2 and C3); 133.6 (C6 and C7); 129.5 (C8a and C10a); 127.7 (C4a and C9a); 126.9 (C5 and C8); 109.3 (C1 and C4); 69.4 (OCH_2); 31.9 (t); 29.6 (t); 29.4 (t); 29.3 (t); 28.9 (t); 25.9 ($OCH_2CH_2CH_2$); 22.7 (OCH_2CH_2); 14.1 (CH_3). FAB^+-MS: m/z (%) 492 (100), 367 (24), 240 (53).

*2,3-Di-n-undecyloxy-9,10-anthraquinone (**3**C_{11}).* Starting from 1.0 g of **4**, compound **3**C_{11} (1.8 g, 79%), m.p. 97 °C (heptane–benzene), was obtained with elution system A. ν_{max} (KBr): 2955, 2922, 2849, 1669, 1576, 1515, 1466, 1378, 1329, 1221, 1113, 713 and 621 cm^{-1}. ^1H NMR ($CDCl_3$): δ 8.26 (2H, m, H5 and H8); 7.74 (2H, m, H6 and H7); 7.67 (2H, s, H1 and H4); 4.18 (4H, t, $J = 6.9$Hz, OCH_2); 1.89 (4H, m, OCH_2CH_2); 1.48 (4H, m, $OCH_2CH_2CH_2$); 1.25 (28H, m, CH_2); 0.87 (3H, t, $J = 6.6$ Hz, CH_3). ^{13}C NMR: δ 182.7 (C9 and C10); 153.5 (C2 and C3); 133.7 (C6 and C7); 133.5 (C8a and C10a); 128.0 (C4a and C9a); 126.9 (C5 and C8); 109.3 (C1 and C4); 69.4 (OCH_2); 32.0 (t); 29.8 (t); 29.7 (t); 29.6 (t); 29.4 (t); 28.9 (t); 26.0 (t); 22.7 (CH_2CH_3); 14.2 (CH_3). FAB^+-MS: m/z (%) 548 (100); 389 (37); 240 (59).

Compounds 1C_n: general procedue for the reduction of anthraquinones 3C_n. In a three-neck round-bottom flask equipped with a reflux condenser, a drying column and a magnetic stirrer, the required amount of 2,3-dialkoxy-9,10-anthraquinone and 2-propanol (20 cm^3 per mmol) were placed and a large excess of sodium borohydride (*ca.* 20 molar equiv.) was added in small portions at such a rate as to avoid a rapid temperature rise. The medium was refluxed under nitrogen for 3 h and allowed to cool to room temperature. The mixture was then hydrolyzed with 35% hydrochloric acid in crushed ice and extracted repeatedly with dichloromethane. The organic layers were combined, washed with a sodium hydroxide solution (pH ≈ 9) and water until neutral, dried ($MgSO_4$) and filtered. The solvent was evaporated and the solid residue (which is the anthrone intermediate), which was not purified further, was treated in the same way, using the same set-up as above, except that the reflux was maintained for *ca.* 12 h. The final residue was chromatographed on a column of silica gel after dissolution in a solvent mixture of CH_2Cl_2–petroleum ether (v/v 30:70). Average yields were 50–60%.

*2,3-Di-n-heptyloxyanthracene (**1**C_7).* Starting from **3**C_7 (0.75 g), 0.39 g (56%) of **1**C_7, m.p. 110 °C, was isolated. Anal. calcd for $C_{28}H_{38}O_2$: C, 82.76; H, 9.36%; found: C, 82.66; H, 9.47%. ν_{max} (KBr): 2951, 2929, 2855, 1627, 1568, 1493, 1465, 1387, 1291, 1261, 1228, 1193, 1166, 1007, 889, 832, 743, 595 and 474 cm^{-1}. ^1H NMR: δ 8.24 (s, H9 and H10); 7.96 (m, H5 and H8); 7.45 (m, H6 and H7); 7.22 (s, H1 and H4); 4.17 (t, $J = 6.4$Hz, OCH_2); 2.00 (m, OCH_2CH_2); 1.58 (m, $OCH_2CH_2CH_2$); 1.43 (m, CH_2); 1.02 (t, $J = 6.4$ Hz, CH_3). ^{13}C NMR: δ 150.2 (C2 and C3); 130.9 (C8a and C10a); 128.9 (C4a and C9a); 127.7 (C5 and C8); 124.4 (C6 and C7); 123.8 (C9 and C10); 106.0 (C1 and C4); 68.8 (OCH_2); 32.0 (t); 29.3 (t); 29.2 (t); 26.2 (CH_2CH_3); 14.2 (CH_3).

*2,3-Di-n-octyloxyanthracene (**1**C_8).* Starting from 0.81 g of **3**C_8, 0.37 g (49%) of **1**C_8, m.p. 105 °C, was obtained. ν_{max} (KBr): 2952, 2930, 2855, 1627, 1568, 1493, 1465, 1387, 1291, 1261, 1230, 1193, 1166, 1006, 889, 832, 743, 595 and 474 cm^{-1}. ^1H NMR: δ 8.22 (s, H9 and H10); 7.95 (m, H5 and H8); 7.43 (m, H6 and H7); 7.20 (s, H1 and H4); 4.17 (t, $J = 6.4$Hz, OCH_2); 1.97 (m, OCH_2CH_2); 1.58 (m, $OCH_2CH_2CH_2$); 1.39 (m, CH_2); 0.96 (t, $J = 6.4$ Hz, CH_3). ^{13}C NMR: δ 150.1 (C2 and C3); 130.8 (C8a and C10a); 128.8 (C4a and C9a); 127.7 (C5 and C8); 124.4 (C6 and C7); 123.8 (C9 and C10); 106.0 (C1 and C4); 68.8 (OCH_2); 31.9 (t); 29.5 (t); 29.4 (t); 29.2 (t); 26.2 (CH_2CH_3); 22.8 (t); 14.2 (CH_3). HRMS: calcd for $C_{30}H_{42}O_2$: 434.3184; found: 434.3148.

*2, 3-Di-n-nonyloxyanthracene (**1**C_9).* Starting from **3**C_9 (1.23 g), 0.64 g (55%) of **1**C_9, m.p. 100 °C, was isolated. Anal. calcd for $C_{32}H_{46}O_2$: C, 83.12; H, 9.96%; found: C, 83.29; H, 9.94%. ν_{max} (KBr): 2953, 2919, 2851, 1629, 1568, 1530, 1491, 1481, 1466, 1384, 1287, 1223, 1165, 1005, 889, and 739 cm^{-1}. ^1H NMR: δ 8.24 (s, H9 and H10); 7.98 (m, H5 and H8); 7.47 (m, H6 and H7); 7.21 (s, H1 and H4); 4.17 (t, $J = 6.6$Hz, OCH_2); 1.99 (m, OCH_2CH_2); 1.58 (m, $OCH_2CH_2CH_2$); 1.25 (m, 20H, CH_2); 0.98 (t, $J = 6.6$ Hz, CH_3). ^{13}C NMR: δ 150.0 (C2 and C3); 130.7 (C8a and C10a); 128.7 (C4a and C9a); 127.6 (C5 and C8); 124.4 (C6 and C7); 123.7 (C9 and C10); 105.9 (C1 and C4); 68.7 (OCH_2); 32.0 ($CH_2CH_2CH_3$); 29.7 (t); 29.5 (t); 29.4 (t); 29.1 (t, OCH_2CH_2); 26.2 (t, $OCH_2CH_2CH_2$); 22.8 (CH_2CH_3); 14.2 (CH_3).

*2, 3-Di-n-undecyloxyanthracene (**1**C_{11}).* Starting from **3**C_{11} (0.73 g), 0.43 g (62%) of **1**C_{11}, m.p. 102–103 °C (pentane), was obtained. ν_{max} (KBr): 2917, 2849, 1630, 1586, 1491, 1481, 1466, 1384, 1287, 1222, 1164, 890 and 739 cm^{-1}. ^1H NMR: δ 8.25 (s, H9 and H10); 7.98 (m, H5 and H8); 7.45 (m, H6 and H7); 7.23 (s, H1 and H4); 4.20 (t, $J = 6.8$Hz, OCH_2); 2.00 (m, OCH_2CH_2); 1.55 (m, $OCH_2CH_2CH_2$); 1.37 (m, CH_2); 0.98 (t, $J = 6.8$ Hz, CH_3). ^{13}C NMR: δ 150.1 (C2 and C3); 130.8 (C8a and C10a); 128.8 (C4a and C9a); 127.6 (C5 and C8); 124.4 (C6 and C7); 123.8 (C9 and C10); 106.0 (C1 and C4); 68.8 (OCH_2); 32.0 ($CH_2CH_2CH_3$); 29.7 (t); 29.5 (t); 29.4 (t); 29.1 (t); 26.2 (t); 22.8 (CH_2CH_3); 14.2 (CH_3). FAB^+-MS: m/z (%) 518 (100); 329 (33); 307 (45); 289 (52); 210 (68). HRMS: calcd for $C_{36}H_{54}O_2$: 518.4123; found 518.4116.

2,3-Trimethylenedioxyanthracene (2$_3$). 2,3-Dihydroxy-9,10-anthraquinone (**4**; 3 g, 12.5 mmol),[50] potassium carbonate (5 g, 36 mmol) and 100 cm^3 DMF were placed in a three-necked round-bottom flask equipped with a dropping funnel and a reflux condenser, under a nitrogen atmosphere. A solution of 1,3-dibromopropane (3 g, 15 mmol) in 50 cm^3 DMF was added slowly through the dropping funnel to the mixture heated at 100 °C. After the addition, the medium temperature was raised to 160 °C and maintained for 17 h. Another aliquot of the anthraquinone solution (0.5 g, 3.6 mmol, in 25 cm^3 DMF) was then added and allowed to react for a further 2 h. After cooling, the reaction mixture was diluted with 300 cm^3 water, which generated a yellowish precipitate that was filtered off and dissolved in CH_2Cl_2, washed with water and dried on Na_2SO_4. After filtration and evaporation of the solvent, the pale brown raw material (**5**$_3$, 2.4 g) was collected to be used in the next step without further purification.

In a round-bottom flask equipped with a reflux condenser, a ground mixture of the crude anthraquinone derivative (**5**$_3$) and zinc powder (5 g, 7.7 mmol) was added to a 20% ammonia

aqueous solution (100 cm^3). The mixture, which rapidly turned dark red, was stirred at 90 °C until the coloration vanished (*i.e.* for about 10 h). The mixture was filtered and the solid was washed with boiling ethanol, dissolved in dichloromethane and chromatographed on a column of silica gel (eluant: CH_2Cl_2–petroleum ether, v/v 50:50). Compound $\mathbf{2}_3$ was isolated as a pale yellow powder (1.1 g, overall yield 35%), m.p. 218 °C. Anal. calcd for $C_{17}H_{14}O_2$: C, 81.60; H, 5.60; O, 12.80%; found: C, 82.22; H, 5.60; O, 12.73%. ν_{max} (KBr): 3040, 2950, 2860, 1475, 1455, 1380, 1300, 1275, 1210, 1135, 1040, 935, 885 and 730 cm^{-1}. ^1H NMR ($CDCl_3$): δ 2.28 (m, 2H); 4.33 (t, 4H); 7.0–8.26 (m, 8H). MS: m/z (%) 250 (M^+, 100), 222 (25), 181 (28), 165 (23), 164 (25), 152 (17), 28 (31).

Appendix: determination of equilibrium constants between solution and gel phase from the phase transition diagrams

At a given temperature, the equilibrium constant of the reversible reaction: gel $\rightleftarrows$ liquid (solution) is expressed by K = activity (liquid)/activity (gel) $\approx a/1$.

The melting of a gel into the liquid phase is assumed to resemble the melting of a solid[66] whose activity is 1. As the concentration of DDOA is low, the activity of the liquid phase will be represented by that of its molar fraction denoted ϕ; therefore:

$$\ln K = \ln\phi \qquad \text{(A1)}$$

where

$$\ln\phi = -\Delta G^0/RT \qquad \text{(A2)}$$

and

$$\ln\phi = -\Delta H^0/R \times 1/T_m + \Delta S^0/R \qquad \text{(A3)}$$

with T_m being the melting temperature.

Conversely, the reversible formation of a gel from the liquid phase (similar to a crystallization) will be represented by $K \approx 1/a$, which leads to:

$$\ln\phi = +\Delta H^0/R \times 1/T_{gel} - \Delta S^0/R \qquad \text{(A4)}$$

where T_{gel} is the gelification temperature. ΔH^0 and ΔS^0 (standard conditions) will be positive for the melting and negative for the gelification. The molar fraction $\phi = x_{solute}/(x_{solute} + x_{solvent})$. As $x_{solute} << x_{solvent}$, $\phi \approx x_{solute}/x_{solvent}$ and therefore, $\phi = (m/M)/(m'/M')$ where m and m' are the masses of solute and solvent, respectively while M and M' are the molar masses.

Acknowledgements

D. Meerschaut is grateful to the CNRS for a postdoctoral grant and to Dr. R. Lesclaux and to University Bordeaux 1 for financial assistance. We thank Dr. M. Lamotte for assistance in gated spectroscopy as well as F. Fages and R. Utermöhlen for valuable discussions. Financial support from the Région Aquitaine is acknowledged with gratitude.

References

1 *Reversible Polymeric Gels and Related Systems*, ed. P. S. Russo, ACS Symposium Series 350, American Chemical Society, Washington, D.C., 1987.
2 *Physical Networks, Polymers and Gels*, eds. W. Buchard and S. B. Ross-Murphy, Elsevier Applied Science, London, 1990.
3 *Food Polymers, Gels and Colloids*, ed. E. Dickinson The Royal Society of Chemistry, Cambridge, UK, 1991.
4 J. M. Guenet, *Thermoreversible Gelation of Polymers and Biopolymers*, Academic Press, London, 1992.
5 J. H. Fuhrhop and W. Helfrich, *Chem. Rev.*, 1993, **93**, 1565.
6 K. te Nijenhuis, *Thermoreversible Networks*, Springer-Verlag, Berlin, 1997.
7 (*a*) T. Tanaka, C. Wang, V. Pande, A. Y. Grosberg, A. English, S. Masamune, H. Gold, R. Levy and K. King, *Faraday Discuss.*, 1996, **102**, 201; (*b*) "Physikalische Chemie der Gele und Netzwerke", guest eds. H. Hoffman, H. Rehage and W. Oppermann, *Ber. Bunsenges Phys. Chem.*, 1998, **102**, 1523–1717.
8 (*a*) M. Jacoby, *Chem. Eng. News*, 1997, **75**(43), 10; (*b*) R. Dagani, *Chem. Eng. News*, 1997, **75**(23), 26.
9 (*a*) P. Terech and R. G. Weiss, *Chem. Rev.*, 1997, **97**, 3133; (*b*) P. Terech, *Ber. Bunsenges. Phys. Chem.*, 1998, **102**, 1630.
10 W. Gu, L. Lu, G. B. Chapman and R. G. Weiss, *Chem. Commun.*, 1997, 543.
11 J. van Esch, S. de Feyter, R. M. Kellog, F. de Schryver and B. L. Feringa, *Chem.-Eur. J.*, 1997, **3**, 1238.
12 R. J. H. Hafkamp, B. P. A. Kokke, I. M. Danke, H. P. M. Geurts, A. E. Rowan, M. C. Feiters and R. J. M. Nolte, *Chem. Commun.*, 1997, 545.
13 J. E. Sohna-Sohna and F. Fages, *Chem. Commun.*, 1997, 327.
14 M. de Loos, J. van Esch, I. Stokroos, R. M. Kellogg and B. L. Feringa, *J. Am. Chem. Soc.*, 1997, **119**, 12 675.
15 C. M. Garner, P. Terech, J. J. Allegraud, B. Mistrot, P. Nguyen, A. de Geyer and D. Rivera, *J. Chem. Soc., Faraday Trans.*, 1998, **94**, 2173.
16 (*a*) S. Yamasaki and H. Tsutsumi, *Bull. Chem. Soc. Jpn.*, 1996, **69**, 561; (*b*) M. Watase and H. Itagaki, *Bull. Chem. Soc. Jpn.*, 1998, **71**, 1457; (*c*) M. Watase, Y. Nakatani and H. Itagaki, *J. Phys. Chem. B*, 1999, **103**, 2366.
17 K. Inoue, Y. Ono, Y. Kanekiyo, T. Ishi-i, K. Yoshihara and S. Shinkai, *Tetrahedron Lett.*, 1998, **39**, 2981.
18 (*a*) R. Oda, I. Huc and S. J. Candau, *Angew. Chem., Int. Ed.*, 1998, **37**, 2689; (*b*) R. Oda, I. Huc, M. Schmutz, S. J. Candau and F. C. MacIntosh, *Nature (London)*, 1999, **399**, 566.
19 Y.-C. Lin and R. G. Weiss, *Macromolecules*, 1987, **20**, 414.
20 Y.-C. Lin, B. Kachar and R. G. Weiss, *J. Am. Chem. Soc.*, 1989, **111**, 5542.
21 Y.-C. Lin and R. G. Weiss, *Liq. Cryst.*, 1989, **4**, 367.
22 I. Furman and R. G. Weiss, *Langmuir*, 1993, **9**, 2084.
23 R. Mukkamala and R. G. Weiss, *J. Chem. Soc. Chem. Commun.*, 1995, 375.
24 P. Terech, I. Furman and R. G. Weiss, *J. Phys. Chem.*, 1995, **99**, 9558.
25 P. Terech, E. Ostuni and R. G. Weiss, *J. Phys. Chem.*, 1996, **100**, 3759.
26 E. Ostuni, P. Kamaras and R. G. Weiss, *Angew. Chem., Int. Ed. Engl.*, 1996, **35**, 1324.
27 (*a*) D. J. Abdallah and R. G. Weiss, *Langmuir*, 2000, **16**, 352; (*b*) D. J. Abdallah, S. A. Sirchio and R. G. Weiss, *Langmuir*, 2000, **16**, 7558; (*c*) A. Ballabh, D. R. Trivedi and P. Dastidar, *Chem. Mater.*, 2003, **15**, 2136.
28 T. Brotin, R. Utermöhlen, F. Fages, H. Bouas-Laurent and J.-P. Desvergne, *J. Chem. Soc., Chem. Commun.*, 1991, 416.
29 (*a*) P. Terech, J.-P. Desvergne and H. Bouas-Laurent, *J. Colloid Interface Sci.*, 1995, **174**, 258; (*b*) P. Terech, I. Furman, R. G. Weiss, H. Bouas-Laurent, J.-P. Desvergne and R. Ramasseul, *Faraday Discuss.*, 1996, **101**, 345.
30 F. Placin, J.-P. Desvergne and F. Cansell, *J. Mater. Chem.*, 2000, **10**, 2147.
31 F. Placin, J.-P. Desvergne and J.-C. Lassègues, *Chem. Mater.*, 2001, **13**, 117.
32 (*a*) G. M. Clavier, J.-L. Pozzo, H. Bouas-Laurent, C. Liere, C. Roux and C. Sanchez, *J. Mater. Chem.*, 2000, **10**, 1725; (*b*) M. Llusar, L. Pidol, C. Roux, J.-L. Pozzo and C. Sanchez, *Chem. Mater.*, 2002, **14**, 5124.
33 T. Kato, T. Kutsuna, K. Yabuuchi and N. Mizoshita, *Langmuir*, 2002, **18**, 7086.
34 (*a*) K. Hanabusa, R. Tanaka, M. Suzuki, M. Kimura and S. Shirai, *Adv. Mater.*, 1997, **8**, 740; (*b*) Y. Hishikawa, K. Sada, R. Watanabe, M. Miyata and K. Hanabusa, *Chem. Lett.*, 1998, 795.
35 (*a*) S. Shinkai and K. Murata, *J. Mater. Chem.*, 1998, **8**, 485; (*b*) K. Yoza, Y. Ono, K. Yoshihara, T. Akao, H. Shinmori, M. Takeuchi, S. Shinkai and D. N. Reinhoudt, *Chem. Commun.*, 1998, 907; (*c*) O. Gronwald and S. Shinkai, *Chem.-Eur. J.*, 2001, **7**, 4328; (*d*) H. Kobayashi, A. Friggeri, K. Koumoto, M. Amaike, S. Shinkai and D. N. Reinhoudt, *Org. Lett.*, 2002, **4**, 1423 and references therein; (*e*) O. Gronwald, E. Snip and S. Shinkai, *Curr. Opin. Colloid Interface Sci.*, 2002, **7**, 148. The lowest concentrations reported for methyl-4,6-*O*-*para*-nitrobenzylidene-α-D-galactopyranoside and methyl-4,6-*O*-α-D-mannopyranoside in alkanes were found to be 0.9–2.5 mM.

36 (*a*) U. Maitra, P. V. Kumar, N. Chandra, L. J. D'Souza, M. D. Prasanna and A. R. Raju, *Chem. Commun.*, 1999, 595; (*b*) U. Maitra, P. V. Kumar, N. M. Sangeetha, P. Babu and A. R. Raju, *Tetrahedron: Asymmetry*, 2001, **12**, 477.

37 (*a*) J. van Esch, F. Schoonbeek, M. De Loos, H. Kooijman, A. L. Spek, R. M. Kellogg and B. L. Feringa, *Chem.-Eur. J.*, 1999, **5**, 937; (*b*) J. van Esch, F. Schoonbeek, M. De Loos, H. Kooijman, A. L. Spek, R. M. Kellogg and B. L. Feringa, *Chem.-Eur. J.*, 1999, **5**, 6445; (*c*) L. N. Lucas, J. van Esch, R. M. Kellogg and B. L. Feringa, *Chem. Commun.*, 2001, 759.

38 G. Clavier, M. Mistry, F. Fages and J. L. Pozzo, *Tetrahedron Lett.*, 1999, **40**, 9021.

39 H. Ihara, M. Yoshitake, M. Takafuji, T. Yamada, T. Sagawa, C. Hirayama and H. Hachisako, *Liq. Cryst.*, 1999, **26**, 1021.

40 L. A. Cuccia, J. M. Lehn, J. C. Homo and M. Schmutz, *Angew. Chem., Int. Ed.*, 2000, **39**, 233.

41 (*a*) L. D. Lu, T. M. Cocker, R. E. Bachman and R. G. Weiss, *Langmuir*, 2000, **16**, 20; (*b*) M. George and R. G. Weiss, *J. Am. Chem. Soc.*, 2001, **123**, 10 393.

42 (*a*) R. Wang, C. Geiger, L. H. Chen, B. Swanson and D. G. Whitten, *J. Am. Chem. Soc.*, 2000, **122**, 2399; (*b*) D. C. Duncan and D. G. Whitten, *Langmuir*, 2000, **16**, 2399.

43 R. P. Lyon and W. M. Atkins, *J. Am. Chem. Soc.*, 2001, **123**, 4408.

44 A. Ajayagosh and S. J. George, *J. Am. Chem. Soc.*, 2001, **123**, 5148.

45 (*a*) J. Makarevic, M. Jokic, B. Peric, V. Tomsic, B. Kojic-Prodic and M. Zinic, *Chem.-Eur. J.*, 2001, **7**, 3328; (*b*) L. Frkanec, M. Jokic, J. Makarevic, K. Wolsperger andZinic, *J. Am. Chem. Soc.*, 2002, **124**, 9716.

46 (*a*) F. M. Menger and K. L. Caran, *J. Am. Chem. Soc.*, 2000, **122**, 11 679; amino acid derivatives were found to rigidify mixtures of H_2O–DMSO at concentrations <0.3 mM; (*b*) M. Kölbel and F. M. Menger, *Chem. Commun.*, 2001, 275; (*c*) M. Kölbel and F. M. Menger, *Langmuir*, 2001, **17**, 4490.

47 Y. Y. Waguespack, S. Barnerjee, P. Ramannair, G. C. Irvin, V. T. John and G. L. McPherson, *Langmuir*, 2000, **16**, 3036.

48 A. J. Carr, R. Melendez, S. J. Geib and A Hamilton, *Tetrahedron Lett.*, 1998, **39**, 7447.

49 C. Shi, Z. Huang, S. Kilic, J. Xu, R. M. Enick, E. J. Beckman, A. J. Carr, R. E. Melendez and A. D. Hamilton, *Science*, 1999, **286**, 1540.

50 J.-L. Pozzo, G. M. Clavier, M. Colomès and H. Bouas-Laurent, *Tetrahedron*, 1997, **53**, 6377; (*b*) 2,3-Dimethoxyanthracene **1**C_1 was first prepared by: V. K. Lagodzinski, *Ann. Chem.*, 1905, **342**, 90.

51 D. Marquis, J.-P. Desvergne and H. Bouas-Laurent, *J. Org. Chem.*, 1995, **60**, 7984.

52 G. Biesmans, G. Verbeek, B. Verschuere, M. van der Auweraer and F. C. de Schryver, *Thin Solid Films*, 1989, **169**, 127.

53 M. van der Auweraer, G. Biesmans and F. C. de Schryver, *Chem. Phys.*, 1988, **119**, 355.

54 J. Ferguson, A. Castellan, J.-P. Desvergne and H. Bouas-Laurent, *Chem. Phys. Lett.*, 1981, **78**, 446.

55 J.-L. Pozzo, J.-P. Desvergne, G. M. Clavier, H. Bouas-Laurent, P. G. Jones and J. Perlstein, *J. Chem. Soc., Perkin Trans. 2*, 2001, 824.

56 F. Placin, J.-P. Desvergne, C. Belin, T. Buffeteau, B. Desbats, L. Ducasse and J. C. Lassègues, *Langmuir*, 2003, **19**, 4563.

57 (*a*) H. Bouas-Laurent, A. Castellan, J.-P. Desvergne and R. Lapouyade, *Chem. Soc. Rev.*, 2000, **29**, 43; (*b*) H. Bouas-Laurent, A. Castellan, J.-P. Desvergne and R. Lapouyade, *Chem. Soc. Rev.*, 2001, **30**, 248; (*c*) H. Bouas-Laurent and J.-P. Desvergne, in *Photochromism, Molecules and Systems* (revised edition), eds. H. Dürr and H. Bouas-Laurent, Elsevier, Amsterdam, 2003, ch. 14, pp 561–630.

58 Y. Ono, K. Nakashima, M. Sano, Y. Kanekiyo, K. Inoue, J. Hojo and S. Shinkai, *Chem. Commun.*, 1998, 1477.

59 J. H. Jung, M. Amaike and S. Shinkai, *Chem. Commun.*, 2000, 2343.

60 K. Murata, M. Aoki, T. Suzuki, T. Harada, H. Kawabata, T. Komori, F. Ohseto, K. Ueda and S. Shinkai, *J. Am. Chem. Soc.*, 1994, **116**, 6664.

61 K. Hanabusa, K. Okui, K. Karaki, M. Kimura and H. Shirai, *J. Colloid Interface Sci.*, 1997, **195**, 86.

62 K. Yoza, N. Amanokura, Y. Ono, T. Akao, H. Shinmori, M. Takeuchi, S. Shinkai and D. N. Rheinhoudt, *Chem.-Eur. J.*, 1999, **5**, 2722.

63 L. N. Lucas, *PhD Thesis*, Groningen, The Netherlands, 2001.

64 F. Lahmani, A. Zehnacker, J.-P. Desvergne, H. Bouas-Laurent, M. Colomès and A. Krueger, *J. Photochem. Photobiol. A*, 1998, **113**, 203.

65 T. Brotin, J. Waluk, J.-P. Desvergne, H. Bouas-Laurent and J. Michl, *Photochem. Photobiol.*, 1992, **55**, 335.

66 (*a*) P. W. Atkins, *Physical Chemistry*, Oxford University Press, 5th edn. 1994, pp. 226–227; (*b*) J. E. Eldridge and J. D. Ferry, *J. Phys. Chem.*, 1954, **58**, 992.